

Multimodel projections and uncertainties of irrigation water demand under climate change

Yoshihide Wada,¹ Dominik Wisser,^{2,3} Stephanie Eisner,⁴ Martina Flörke,⁴ Dieter Gerten,⁵ Ingjerd Haddeland,⁶ Naota Hanasaki,⁷ Yoshimitsu Masaki,⁷ Felix T. Portmann,^{8,9} Tobias Stacke,¹⁰ Zachary Tessler,¹¹ and Jacob Schewe⁵

Received 9 April 2013; revised 28 May 2013; accepted 19 June 2013; published 10 September 2013.

[1] Crop irrigation is responsible for 70% of humanity's water demand. Since the late 1990s, the expansion of irrigated areas has been tapering off, and this trend is expected to continue in the future. Future irrigation water demand (IWD) is, however, subject to large uncertainties due to anticipated climate change. Here, we use a set of seven global hydrological models (GHMs) to quantify the impact of projected global climate change on IWD on currently irrigated areas by the end of this century, and to assess the resulting uncertainties arising from both the GHMs and climate projections. The resulting ensemble projections generally show an increasing trend in future IWD, but the increase varies substantially depending on the degree of global warming and associated regional precipitation changes. Under the highest greenhouse gas emission scenario (RCP8.5), IWD will considerably increase during the summer in the Northern Hemisphere (>20% by 2100), and the present peak IWD is projected to shift one month or more over regions where $\geq 80\%$ of the global irrigated areas exist and 4 billion people currently live. Uncertainties arising from GHMs and global climate models (GCMs) are large, with GHM uncertainty dominating throughout the century and with GCM uncertainty substantially increasing from the midcentury, indicating the choice of GHM outweighing by far the uncertainty arising from the choice of GCM and associated emission scenario.

Citation: Wada, Y., et al. (2013), Multimodel projections and uncertainties of irrigation water demand under climate change, *Geophys. Res. Lett.*, 40, 4626–4632, doi:10.1002/grl.50686.

Additional supporting information may be found in the online version of this article.

¹Department of Physical Geography, Utrecht University, Utrecht, Netherlands.

²Center for Development Research, University of Bonn, Bonn, Germany.

³Institute for the Study of Earth, Oceans, and Space, University of New Hampshire, Durham, New Hampshire, USA.

⁴Center for Environmental Systems Research, University of Kassel, Kassel, Germany.

⁵Potsdam Institute for Climate Impact Research, Potsdam, Germany.

⁶Norwegian Water Resources and Energy Directorate, Oslo, Norway.

⁷National Institute for Environmental Studies, Tsukuba, Japan.

⁸Biodiversity and Climate Research Center (LOEWE BiK-F) and Senckenberg Research Institute and Natural History Museum, Frankfurt, Germany.

⁹Institute of Physical Geography, Goethe University Frankfurt, Frankfurt, Germany.

¹⁰Max Planck Institute for Meteorology, Hamburg, Germany.

¹¹Environmental CrossRoads Initiative, The City College of New York, New York, USA.

Corresponding author: Y. Wada, Department of Physical Geography, Utrecht University, Postbus 80.115, 3508 TC Utrecht, Netherlands. (y.wada@uu.nl)

©2013. American Geophysical Union. All Rights Reserved.
0094-8276/13/10.1002/grl.50686

1. Introduction

[2] The irrigation sector uses by far the largest amount of water among all sectors and is responsible for 70% of the global water demand (~water withdrawals), sustaining 40% of the global food production [Abdullah, 2006]. For some countries, such as India, Pakistan, Iran, and Mexico, where irrigation sustains much of food production and the livelihood of millions of people, irrigation water demand (IWD) even exceeds 90% of the total water demand [Fischer et al., 2007]. Globally, the area equipped for irrigation, grew sixfold from 0.5 million km² to 3.0 million km², nearly the size of India, between 1900 and 2005 [Freydank and Siebert, 2008]. This expansion occurred rapidly at a rate of nearly 5% per year during the period 1950s–1980s, but it has slowed down since the late 1990s when the growth rate decreased to <1% per year. For the coming decades, the global area of irrigated land is not expected to expand dramatically due to limited land and water available [Faurès et al., 2002; Turrall et al., 2011].

[3] Future IWD is subject to large uncertainties due to anticipated climate change, i.e., increasing temperature and changing precipitation variability, in most regions of the world. Several global studies have quantified the impact of climate change on future IWD [Fischer et al., 2007; Döll, 2002; Pfister et al., 2011; Konzmann et al., 2013] (see auxiliary introduction and Table S1), but their results indicate substantial variations of IWD among different global hydrological models (GHMs) and among different climate projections (global climate models (GCMs)) used to force GHMs. Due to the large GHM- and GCM-specific uncertainty, Gosling et al. [2011] and Haddeland et al. [2011] suggest a multimodel and multiclimate forcing approach to assess climate change impacts. Several studies have shown that the ensemble mean or median is often closer to the observations compared to simulation by individual models, suggesting that multimodel assessments are imperative [Dirmeyer et al., 2006; Guo et al., 2007]. No study has yet used a multi-GHM and multi-GCM approach to analyze IWD globally and to assess the respective uncertainties. Furthermore, little is known about climate change impacts on possible future change of seasonal IWD.

2. Models, Data, and Methods

[4] An ensemble of seven state-of-the-art GHMs: H08 [Hanasaki et al., 2008a, 2008b], LPJmL [Rost et al., 2008; Konzmann et al., 2013], MPI-HM [Hagemann and Gates, 2003; Stacke and Hagemann, 2012], PCR-GLOBWB [Wada et al., 2011a, 2011b], VIC [Liang et al., 1994; Haddeland et al., 2006], WaterGAP [Döll and Siebert, 2002; Portmann

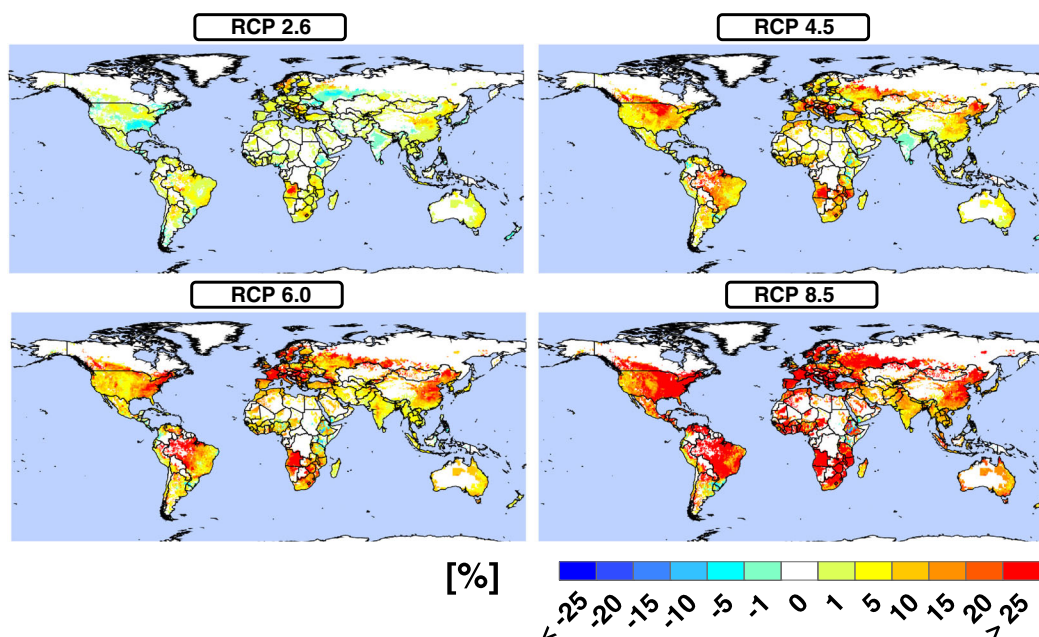


Figure 1. Relative change (%) of IWD by the end of this century (2080s), compared to the present (2000s). The results of the ensemble mean for each RCP (25 ensemble members: five GHMs and five GCMs) are provided.

et al., 2013], WBMplus [Wisser *et al.*, 2008, 2010] was used to quantify globally the impact of climate change on annual and seasonal IWD by the end of this century. We examined the poorly understood uncertainty of future IWD arising from GHMs, the multiclimate change projections, and the underlying emission scenarios (here accounted for by using four Representative Concentration Pathways or RCPs; see auxiliary introduction). The newly available CMIP5 climate projections were obtained through the Inter-Sectoral Impact Model Intercomparison Project (ISI-MIP). The main characteristics of the GHMs, the irrigation inputs and outputs, the CMIP5 climate projections, and the RCPs are given in Tables S2, S3, S4, and S5, respectively. Note that we account only for climate impacts without analyzing socio-economic scenarios of increased demand for food and, thus, IWD. All simulations are forced by the areas currently equipped for irrigation. The crop-related data including the type of crops and crop calendar is assumed to remain constant except for H08 and LPJmL which simulate crop calendar according to daily weather patterns during the simulation period. Changes in projected IWD therefore reflect GCM and scenario projected changes in climate variables (Table S2).

[5] IWD equals the amount of water that needs to be supplied to ensure optimal crop growth considering the losses during water transport and application. In brief, the GHMs simulate IWD per unit crop area based on surface water balance (e.g., surface water layer for paddy rice) and soil water balance (e.g., soil moisture deficit in the root zone calculated from the difference between the water content at field capacity and the water content at wilting point) or depending on the difference between potential evapotranspiration and actual crop evapotranspiration (soil moisture availability) during the crop growing season at a daily time step and a spatial resolution of 0.5° grid (~ 50 km by ~ 50 km at the equator). Water is assumed to be available to fully meet the demand. H08 and LPJmL simulate crop calendar,

growing season length, and crop factor based on climate forcing, whereas the other models prescribe these features using data obtained from various sources [e.g., Portmann *et al.*, 2010; Siebert and Döll, 2010]. The losses during water transport and irrigation application are included in the calculation of IWD, but the parameterization of these losses differs among the GHMs. H08, LPJmL, WaterGAP, and WBMplus use irrigation or project efficiency taken from available country statistics [Döll and Siebert, 2002; Rohwer *et al.*, 2007; Rost *et al.*, 2008], whereas PCR-GLOBWB calculates daily evaporative and percolation losses per unit crop area based on surface and soil water balance [Wada *et al.*, 2013]. Irrigation efficiency typically ranges from 0.3 to 0.8 depending on a type of irrigation (e.g., drip, sprinkler, surface irrigation) and associated conveyance efficiency. Irrigation water consumption (IWC) equals the net amount of irrigation water (without losses) applied during the crop growing season. H08, LPJmL, WaterGAP, and WBMplus divide this amount by irrigation efficiency to calculate IWD, whereas for PCR-GLOBWB, IWC equals the amount of IWD that is actually consumed by irrigated crops, susceptible to the amount of soil moisture. MPI-HM and VIC calculate only IWC.

[6] The GCM climate forcing was bias corrected on a grid-by-grid basis (0.5° grid) by scaling the long-term monthly means of the GCM daily fields to those of the observation-based WATCH climate forcing for the overlapping reference climate 1960–1999 [Hempel *et al.*, 2013] (see auxiliary introduction). Potential evapotranspiration was calculated with the bias-corrected GCM climate forcing, but the method (e.g., temperature and radiation) differs among the GHMs (Table S2). The resulting bias-corrected transient daily climate fields were used to force the seven GHMs to simulate IWD and IWC over the period 1971–2099 with a spin-up, reflecting a climate representative prior to the start of the simulation period. Note that IWD was simulated by

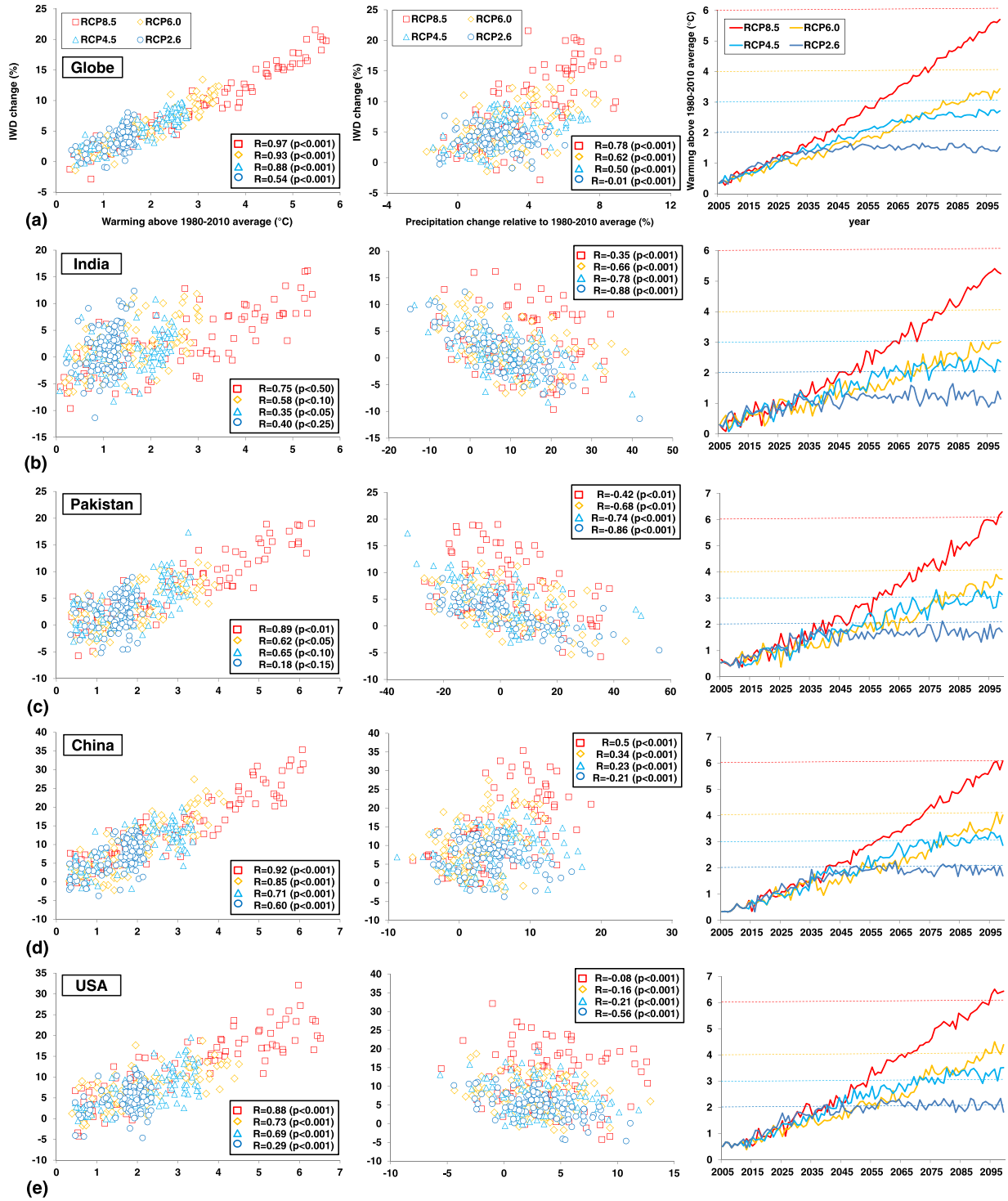


Figure 2. (left) Relative change (%) of IWD (ensemble mean of each RCP) as a function of warming (°C) and (middle) relative change of annual precipitation amounts (%) over (a) the global land and the major irrigated countries: (b) India, (c) Pakistan, (d) China, and (e) the USA. (right) Global warming and warming over each country (°C) are also provided. Changes were calculated relative to the 1980–2010 average for each year from 2005 to 2100. The degree of warming and the amount of precipitation were calculated over the global land and for each country respectively. R and p denote the correlation coefficient and p -value (significance), respectively. The dashed lines represent the warming targets of each RCP.

five GHMs (H08, LPJmL, PCR-GLOBWB, WaterGAP, and WBMplus), whereas IWC was simulated by all GHMs. As a result, 25 (five GHMs by five GCMs) and 35 (seven GHMs by five GCMs) ensemble projections were produced for

IWD and IWC, respectively, under each RCP scenario. The result of each GHM is treated equally, and no weight is given to a particular GHM based on the performance. To evaluate the model performance, a comparison of ensemble mean of

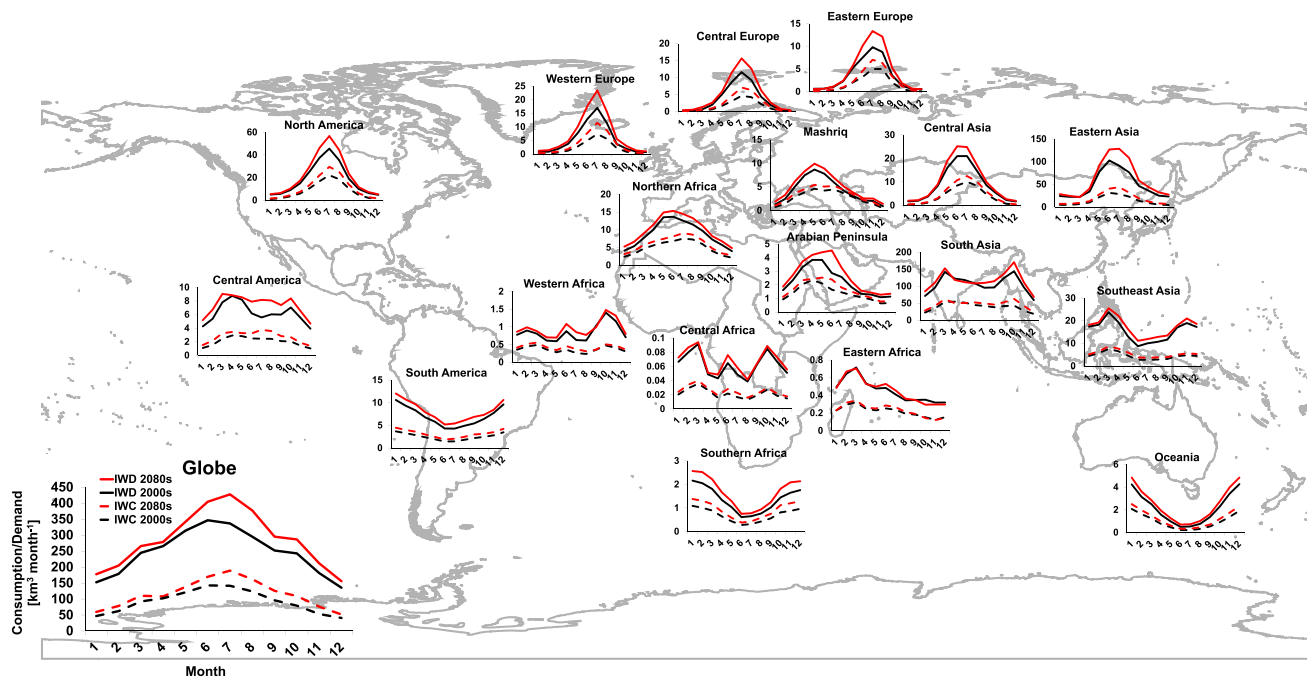


Figure 3. Seasonal IWD (solid line) and IWC (dashed line) for the 2000s (black line) and the 2080s (red line), respectively, under RCP8.5. Ensemble mean was calculated for each region over 18 out of 23 regions (five regions were omitted due to nonirrigated croplands) defined by the UNEP GEO subregions. Global figure is shown at the left corner.

simulated present IWD to reported statistics per country is given in Figure S1 and the auxiliary results.

3. Results

3.1. Projected Changes in IWD

[7] Figure 1 shows the relative change of projected IWD by the end of century (2080s: mean of 2069–2099), compared to the present (2000s: mean of 1980–2010). Under RCP 2.6, IWD (ensemble mean) on average decreases over South Asia including the Indus and the Ganges, Eastern Europe, Southeastern USA, and parts of the Middle East and Africa by 2080s, but increases slightly over other regions of the world (<5%). Under RCP 4.5, IWD increases (>10%) on most irrigated areas except a few regions including South Asia and parts of Eastern Europe and Africa where IWD slightly decreases (<5%). For RCP 6.0, the increase in IWD is substantial (>20%) for China, Europe, and Southern Africa, and becomes even larger for RCP 8.5, under which scenario it exceeds 25% in many heavily irrigated regions in the USA, Europe, many parts of Asia, and Africa. The increase is also obvious from long-term temporal signals of ensemble IWD projections (Figure S2). Global IWD (ensemble of all RCPs) increases by ~10% by midcentury (2050s: mean of 2035–2065), and by ~14% by the 2080s (Table S6). Projected global IWD exhibits the largest increase under RCP8.5, and it increases by ~12% by the 2050s and by ~21% by the 2080s. Under RCP2.6, global IWD increases by ~9% by the 2050s, but afterwards the increase subsides by the 2080s. Among major irrigated countries, IWD (ensemble of all RCPs) for India and Pakistan barely increases by the 2050s, but increases by ~5% by the 2080s. For China, IWD shows the strongest signal and consistently increases by the 2080s (~20%). For the USA, the increase in IWD follows

the global signal. For China and the USA, the ensemble mean of RCP 8.5 projections tends to diverge from other scenarios from the 2050s, whereas for India and Pakistan the ensemble RCP projections follow a similar trend among one another with a large inter-annual variability.

3.2. The Impact of Projected Changes in Temperature and Precipitation

[8] To investigate the impact of projected changes in temperature and precipitation on IWD, in Figure 2, we plotted for each ensemble RCP the relative change of IWD from the present at different levels of mean global warming ($^{\circ}\text{C}$) and to relative change of mean annual precipitation amounts (%) (see Table S7 for calculated statistics). In order to reflect regional variability, the degree of warming and the amount of precipitation change were calculated for individual countries. To relate the corresponding warming over each country to global warming, a warming relative to 1980–2010 average is also plotted for each country. Results show a quasi-linear trend between increasing global IWD and global warming. Correlation between global IWD and global warming increases when warming is higher. Increasing global temperatures generally enhance evaporative demand, leading to higher crop evapotranspiration. Importantly, the impact of warming outweighs the effect of increasing precipitation. Conversely, for India and Pakistan, increasing temperatures do not always lead to rising IWD. Increasing precipitation in the monsoon climate correlates with decreasing IWD, wherever such an increase is projected, mostly overcompensating any temperature effect. In fact, relative increase in precipitation amount is projected to be larger over these countries compared to other major irrigated countries, outweighing the impact of warming (Figure 1). However, above 4°C warming (RCP8.5), IWD tends to increase with rising temperature, canceling out the

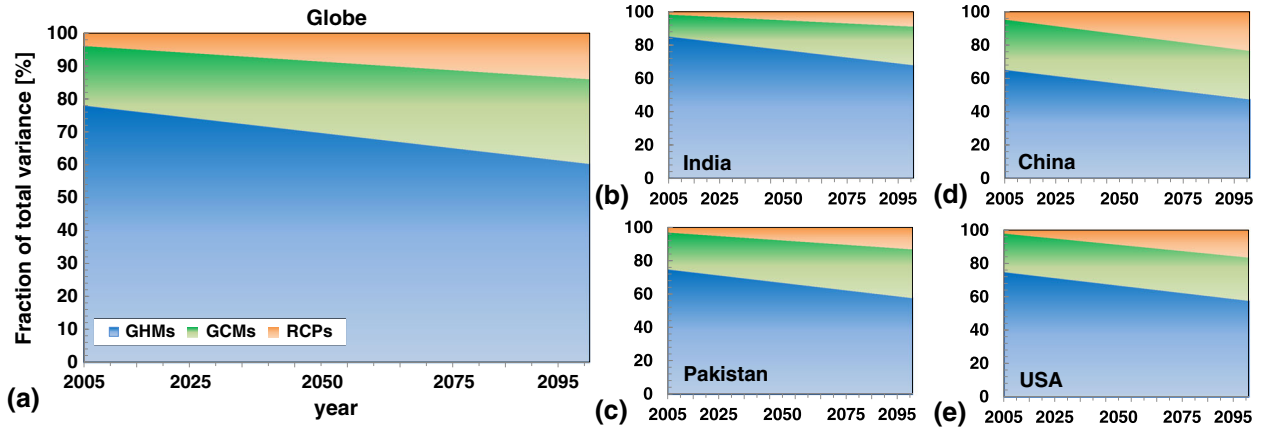


Figure 4. Fraction of total variance (%) in ensemble IWD projection (2005–2100) arising from three distinct sources (see auxiliary methods): GHMs (hydrological models), GCMs (climate models), and RCPs (emission scenarios) [Hawkins and Sutton, 2009] over (a) the globe and for (b) India, (c) Pakistan, (d) China, and (e) the USA.

effect of increasing precipitation. For China and the USA, IWD increases with rising temperature, and no meaningful relationship between IWD and the amount of changing precipitation is found. This may be explained by the substantial climatic range, i.e., arid to humid climate, within these countries.

[9] To highlight the impact of the highest greenhouse gas emission scenario on the seasonal pattern of global and regional IWD, Figure 3 shows ensemble means of monthly IWD and IWC under RCP8.5 scenario projection for the UNEP GEO subregions (<http://www.unep.org/>). Due to pronounced warming and associated precipitation changes, IWD and IWC increase over most of the regions including North and Central America, Europe, and Asia. The increase is considerable during the summer from May to September in the Northern Hemisphere (>20%), but the increase is uneven due to region-specific rise in temperature and associated change in precipitation amounts (Figure 2). Importantly, the peak IWD and IWC are projected to shift by approximately a month later over Eastern Asia (June to July), Arabian Peninsula (May to July), and Northern Africa (May to June), whereas these peaks occur about one month earlier over Central America (April to March) and Central Asia (July to June). The former trend is also obvious for the global signal (June to July). Over South Asia where regional IWD exceeds a quarter of the global total, both IWD and IWC slightly decrease during April to June, but increase in the other seasons. This shifts the peak IWD from March to October (due to multicropping). These results indicate regional averages, but a large variability is observed for shift in peak IWD and IWC within each region (Figure S3). Compared to the regional averages, opposite signals of shift in the peak IWD and IWC are obvious over Northern and Southern China, Pakistan, and Mexico.

3.3. Fractional Uncertainty of GHMs, GCMs, and RCPs

[10] The above results reveal ensemble averages. However, the uncertainties arising from the GHMs and GCMs are substantial over many regions (Figure S4). The range of maximum and minimum of ensemble IWD projections indicates a large spread among the GHMs and the spread increases towards 2100 (Figure S2). Figure S5 shows the model-specific response in global IWD and IWC at different levels of

global warming. A distinct decreasing trend is projected by LPJmL, a model that considers CO₂ fertilization effects on crop photosynthesis and transpiration, while the other GHMs project a consistent increase in both IWD and IWC (similar to LPJmL without CO₂ fertilization effect). The spread among GHMs responding to different degree of global warming is large, suggesting that a large fraction of the spread of ensemble projections is attributed to the differences among the GHMs rather than among the GCMs. Figure 4 indicates the fractional (relative) uncertainty arising from the GHMs, GCMs, and RCPs over the period 2005–2099 relative to the period 1971–2005. The uncertainty from the different GHMs dominates the uncertainty in the global IWD projections throughout the century. The uncertainty of the climate (GCMs) and the scenario (RCPs) projections enlarges towards 2100, due to an increasing variability in precipitation and temperature projections among different RCPs and GCMs. The GHM uncertainty decreases relative to the other uncertainties, but in absolute sense it remains mostly constant over time since the basic model parameters are fixed at the present. The proportion of each fractional uncertainty varies considerably over the different countries. For instance, the RCP uncertainty is higher for China due to a larger variability in climate projections (e.g., precipitation) arising from different emission scenarios from different GCMs. Note that the climatic bias correction may have affected the results of the GCM and RCP uncertainty, by reducing inter-GCM and RCP variability (see auxiliary introduction).

4. Discussion and Conclusions

[11] Our multimodel and multiclimate projections indicate that climate change alone will have substantial impacts on future IWD. Under the highest greenhouse gas emission scenario (RCP8.5), future IWD increases considerably (>20% by 2100) from May to September over North and Central America, and most of Asia where more than 80% of the global irrigated areas exist and 4 billion people currently live. Over South, Central, and Eastern Asia, the Arabian Peninsula, Northern Africa, and Central America, peak IWD is projected to shift by one month or more, triggering a shift in global seasonal IWD signal. The most

likely reason for this shift comes from season-specific changes in temperature and precipitation patterns, which affect seasonal crop calendars simulated by H08 and LPJmL. The other GHMs prescribe a present crop calendar, such that a change in peak IWD is driven solely by projected change in climate patterns. Irrespective of the underlying mechanism, both approaches indicate that climate change not only increases IWD, but also shifts its seasonality. Although our results provide potential demands that are constrained by neither surface freshwater availability nor fossil groundwater abstraction, the net increase and the shift in peak IWD likely has an adverse effect over those irrigated regions where freshwater resources are presently under considerable stress during the summer and major crop growing season (May–September) [Gerten *et al.*, 2007]. This casts significant doubt on the sustainability of regional food production by 2100 [Foley *et al.*, 2011]. However, our modeling approach does not fully reflect regional irrigation practice in which farmers may adapt to changing weather patterns in order to reduce the peak demands, which results in different cropping calendars (e.g., different sowing times and crop growing seasons and length).

[12] Managing IWD facilitates adaptive responses to cope with limited water availability. Sustainable water and land management practices have a potential to improve irrigation efficiency, which will in turn lower the substantial amount of water needed for irrigation. Technological improvements also have the potential to reduce water demands in many rapidly developing countries where water is scarce. Such socio-economic and technological changes are not considered in this study but may play an important role in constraining future IWD. Conversely, with growing world population and altering lifestyles and dietary habits, food consumption is likely to grow as well, such that our estimates of future IWD—projected to change solely in response to climate (and CO₂) change over areas presently equipped for irrigation—are likely to be a minimal change of what can be expected in the future [cf., Fischer *et al.*, 2007; Pfister *et al.*, 2011]. Moreover, as shown by the LPJmL model, increasing atmospheric CO₂ concentration may have a strong beneficial effect on crop growth and crop transpiration (Figure S5). The increase in atmospheric CO₂ concentration improves the water use efficiency of irrigated crops: a higher CO₂ concentration reduces transpiration at the leaf level (physiological effect), while the consequent increase in primary production leads to higher transpiration at the regional scale (structural CO₂ effect) [Betts *et al.*, 1997; Leipprand and Gerten, 2006]. Field and laboratory studies show the positive beneficial CO₂ effect (lower crop transpiration), but only to the extent that other factors—in particular nutrient supply—are not limiting crop growth [Konzmann *et al.*, 2013]. However, it remains disputed whether the CO₂-induced lower crop transpiration due to improved water use efficiency may be canceled out by higher crop transpiration as a result of simultaneously increased biomass. Thus, the CO₂ effect on regional and global IWD remains uncertain. Although the uncertainty in ensemble IWD projections remains large, climate change alone likely increases IWD in many regions of the world. Such increase will bring a further challenge for local farmers to cope with finite water resources for food production. However, the magnitude of the increase largely relies on the degree of global warming and associated precipitation patterns.

[13] **Acknowledgments.** We thank three anonymous reviewers for their constructive comments, which substantially improved the manuscript. This work has been conducted under the framework of ISI-MIP funded by the German Federal Ministry of Education and Research (BMBF) (Project funding reference number: 01LS1201A). The authors acknowledge the World Climate Research Program's Working Group on Coupled Modelling responsible for CMIP and the climate modeling groups (Table S4) for their model outputs. For CMIP the U.S. Department of Energy's Program for Climate Model Diagnosis and Intercomparison provided coordinating support and led development of software infrastructure in partnership with the Global Organization for Earth System Science Portals. Y.W. was supported by Research Focus Earth and Sustainability of Utrecht University (Project FM0906: Global Assessment of Water Resources). N.H. and Y.M. were supported by the Environment Research and Technology Development Fund (S-10) of the Ministry of the Environment, Japan.

[14] The Editor thanks Stephan Pfister and two anonymous reviewers for their assistance in evaluating this manuscript.

References

- Abdullah, K. B. (2006), Use of water and land for food security and environmental sustainability, *Irrig. Drain.*, 55, 219–222.
- Betts, R. A., et al. (1997), Contrasting physiological and structural vegetation feedbacks in climate change simulations, *Nature*, 387, 796–799.
- Dirmeier, P., et al. (2006), GSWP-2–Multimodel analysis and implications for our perception of the land surface, *Bull. Am. Meteorol. Soc.*, 87, 1381–1397.
- Döll, P. (2002), Impact of climate change and variability on irrigation requirements: A global perspective, *Clim. Change*, 54, 269–293.
- Döll, P., and S. Siebert (2002), Global modeling of irrigation water requirements, *Water Resour. Res.*, 38(4), 1037, doi:10.1029/2001WR000355.
- Faurès, J. M., et al. (2002), The FAO irrigated area forecast for 2030, Food and Agric. Organ., Rome.
- Fischer, G., et al. (2007), Climate change impacts on irrigation water requirements: Effects of mitigation, 1990–2080, *Technol. Forecasting Soc. Change*, 74, 1083–1107.
- Foley, J. A., et al. (2011), Solutions for a cultivated planet, *Nature*, 478, 337–342.
- Freydank, K., and S. Siebert (2008), Towards mapping the extent of irrigation in the last century: A time series of irrigated area per country, *Frankfurt Hydrol. Pap.*, 08., Univ. of Frankfurt, Frankfurt, Germany.
- Gerten, D., et al. (2007), Potential future changes in water limitation of the terrestrial biosphere, *Clim. Change*, 80, 277–299.
- Gosling, S. N., et al. (2011), A comparative analysis of projected impacts of climate change on river runoff from global and catchment-scale hydrological models, *Hydrol. Earth Syst. Sci.*, 15, 279–294.
- Guo, Z., et al. (2007), Improving the quality of simulated soil moisture with a multi-model ensemble approach, *Q. J. R. Meteorol. Soc.*, 133, 731–747.
- Haddeland, I., et al. (2006), Anthropogenic impacts on continental surface water fluxes, *Geophys. Res. Lett.*, 33, L08406, doi:10.1029/2006GL026047.
- Haddeland, I., et al. (2011), Multimodel estimate of the global terrestrial water balance: Setup and first results, *J. Hydrometeorol.*, 12, 869–884.
- Hagemann, S., and L. D. Gates (2003), Improving a sub-grid runoff parameterization scheme for climate models by the use of high resolution data derived from satellite observations, *Clim. Dyn.*, 21, 349–359.
- Hanasaki, N., et al. (2008a), An integrated model for the assessment of global water resources—Part 1: Model description and input meteorological forcing, *Hydrol. Earth Syst. Sci.*, 12, 1007–1025.
- Hanasaki, N., et al. (2008b), An integrated model for the assessment of global water resources—Part 2: Applications and assessments, *Hydrol. Earth Syst. Sci.*, 12, 1027–1037.
- Hawkins, E., and R. Sutton (2009), The potential to narrow uncertainty in regional climate predictions, *Bull. Am. Meteorol. Soc.*, 90, 1095–1107.
- Hempel, S., et al. (2013), A trend-preserving bias correction—the ISI-MIP approach, *Earth Syst. Dyn. Discuss.*, 4, 49–92.
- Konzmann, M., et al. (2013), Climate impacts on global irrigation requirements under 19 GCMs, simulated with a vegetation and hydrology model, *Hydrol. Sci. J.*, 58, 88–105.
- Leipprand, A., and D. Gerten (2006), Global effects of doubled atmospheric CO₂ content on evapotranspiration, soil moisture, and runoff, *Hydrol. Sci. J.*, 51, 171–185.
- Liang, X., D. P. Lettenmaier, E. F. Wood, and S. J. Burges (1994), A simple hydrologically based model of land surface water and energy fluxes for general circulation models, *J. Geophys. Res.*, 99(D7), 14,415–14,428, doi:10.1029/94JD00483.
- Pfister, S., et al. (2011), Projected water consumption in future global agriculture: Scenarios and related impacts, *Sci. Total Environ.*, 409, 4206–4216.
- Portmann, F. T., et al. (2010), MIRCA2000–Global monthly irrigated and rainfed crop areas around the year 2000: A new high-resolution data set

- for agricultural and hydrological modelling, *Global Biogeochem. Cycles*, 24, GB1011, doi:10.1029/2008GB003435.
- Portmann, F. T., et al. (2013), Impact of climate change on renewable groundwater resources: Assessing the benefits of avoided greenhouse gas emissions using selected CMIP5 climate projections, *Environ. Res. Lett.*, 8, 024023.
- Rohwer, J., D. Gerten, and W. Lucht (2007), Development of functional types of irrigation for improved global crop modelling, *PIK Rep. 104*, Potsdam Institute for Climate Impact Research (PIK), Potsdam, Germany.
- Rost, S., et al. (2008), Agricultural green and blue water consumption and its influence on the global water system, *Water Resour. Res.*, 44, W09405, doi:10.1029/2007WR006331.
- Siebert, S., and P. Döll (2010), Quantifying blue and green virtual water contents in global crop production as well as potential production losses without irrigation, *J. Hydrol.*, 384, 198–217.
- Stacke, T., and S. Hagemann (2012), Development and evaluation of a global dynamical wetlands extent scheme, *Hydrol. Earth Syst. Sci.*, 16, 2915–2933.
- Turrall, H., et al. (2011), Climate change, water and food security, *Water Rep.*, 36, Food and Agric. Organ., Rome.
- Wada, Y., et al. (2011a), Modelling global water stress of the recent past: On the relative importance of trends in water demand and climate variability, *Hydrol. Earth Syst. Sci.*, 15, 3785–3808.
- Wada, Y., et al. (2011b), Global monthly water stress: 2. Water demand and severity of water, *Water Resour. Res.*, 47, W07518, doi:10.1029/2010WR009792.
- Wada, Y., et al. (2013), Global modeling of withdrawal, allocation and consumptive use of surface water and groundwater resources, *Earth Syst. Dyn. Discuss.*, 4, 355–392.
- Wisser, D., et al. (2008), Global irrigation water demand: Variability and uncertainties arising from agricultural and climate data sets, *Geophys. Res. Lett.*, 35, L24408, doi:10.1029/2008GL035296.
- Wisser, D., B. M. Fekete, C. J. Vörösmarty, and A. H. Schumann (2010), Reconstructing 20th century global hydrography: A contribution to the Global Terrestrial Network-Hydrology(GTN-H), *Hydrol. Earth Syst. Sci.*, 14, 1–24, doi:10.5194/hess-14-1-2010.